Current Research (2025) Newfoundland and Labrador Department of Industry, Energy and Technology Geological Survey, Report 25-1, pages 115-130

METASEDIMENTARY SEQUENCES IN THE LONG RANGE INLIER: DETRITAL ZIRCON EVIDENCE FOR POST-GRENVILLIAN SEDIMENTARY DEPOSITION

A.M. Hinchey, S. Serna Ortiz, D. Skipton and D. Mendoza Marin
Regional Geology Section

ABSTRACT

*The Long Range Inlier in western Newfoundland is a Proterozoic basement massif within the Appalachian orogen that preserves a complex geological history. Part of the inlier comprises the Long Range Gneiss Complex, defined by several phases of orthogneiss, and rare, thin sequences of paragneiss. The provenance of the metasedimentary sequences was ambiguous, with the depositional ages interpreted as older than the Pinwarian orogeny (>1500 Ma), and, in part, as Neoproterozoic to Ordovician. U–Pb detrital zircon analyses were conducted on three samples from two metasedimentary sequences, revealing distinct depositional ages and provenance signatures. A sample of Sequence A, flanking the Taylor Brook Gabbro Suite, yields a maximum depositional age of 554 ± 15 Ma, consistent with Cambro-Ordovician sequences of the Laurentian cover sequence. A second sample from Sequence A yields a maximum depositional age of 996 ± 26 Ma, consistent with sediment derived from the Grenvillian basement. Sequence B, previously interpreted as comprising the oldest (*i.e.*, Pinwarian orogen) part of the Long Range Gneiss Complex, yields a maximum depositional age of 906 ± 7 Ma, indicating post-Grenvillian source material. The detrital signature of Sequence B suggests either a post-Grenvillian rifting event, creating a basin* ca. *900 Ma, perhaps related to the opening of the Asgard Sea, or that Sequence B is also part of the Laurentian cover sequence. The detrital signatures indicate locally fed, isolated depositional basins with varying contributions from Grenvillian, Paleoproterozoic, and Archean sources. Based on their detrital signatures, all three samples could be part of the Laurentian cover sequence. The study challenges existing stratigraphic interpretations, underscoring the need for further detrital geochronology to refine the tectonic and sedimentary history of the region.*

INTRODUCTION

Newfoundland is divided from west to east into four tectonostratigraphic zones; the Humber, Dunnage (Notre Dame/Dashwoods and Exploits subzones), Gander and Avalon zones based on lithological, paleontological and lithogeochemical contrasts in pre-Silurian rocks. The Humber Zone (or margin, *see* van Staal and Barr, 2012) consists of crystalline basement rocks of the Grenville Province (Long Range Inlier) that are unconformably overlain by a cover sequence containing (from bottom to top) rift-related, passive-continental-margin, and foreland-basin units that are, in places, structurally overlain by a transported succession (Taconian allochthons). The allochthons contain formations equivalent to the cover sequence and are overlain by ophiolitic rocks (Figure 1). In the surveyed areas, the Laurentian cover sequence includes both autochthonous and allochthonous rocks. The Humber margin is divided into a western external domain and an eastern internal domain based on the increasing deformation and metamorphism to the east. The basement rocks (Long Range Inlier) are interpreted as part of the Pinware terrane of the Grenville orogen (Heaman *et al.*, 2002).

The southern part of the Long Range Inlier comprises part of the Silver Mountain map area (NTS 12H/11; Hinchey, 2020) and includes two metasedimentary sequences that are the focus of this study (Figure 2). A sequence of three sedimentary units, herein referred to as Sequence A, is preserved flanking the edges of the Taylor Brook Gabbro Suite (TBGS). This sequence was initially interpreted as being older than the Pinwarian orogeny (>1550 Ma, Owen, 1991); however, based on the simple deformation history and low grade of metamorphism preserved in the sequence, Hinchey (2010) suggested it was Neoproterozoic to Paleozoic and part of the Laurentian cover sequence. This sequence includes thin psammite, marble and semipelite to quartzite units. The psammite layer was the focus of this study. A second metasedimentary sequence, herein referred to as Sequence B, consists of interlayered quartzite and psammite. This sequence was previously interpreted as being part of the Long Range Gneiss Complex and was thought to be part of the Pinware terrane (>1550 Ma), potentially representing some of the oldest preserved rocks in the region (Owen, 1991). This report tests these hypotheses by providing detrital U–Pb zircon analyses from two samples of Sequence A and one sample from Sequence B.

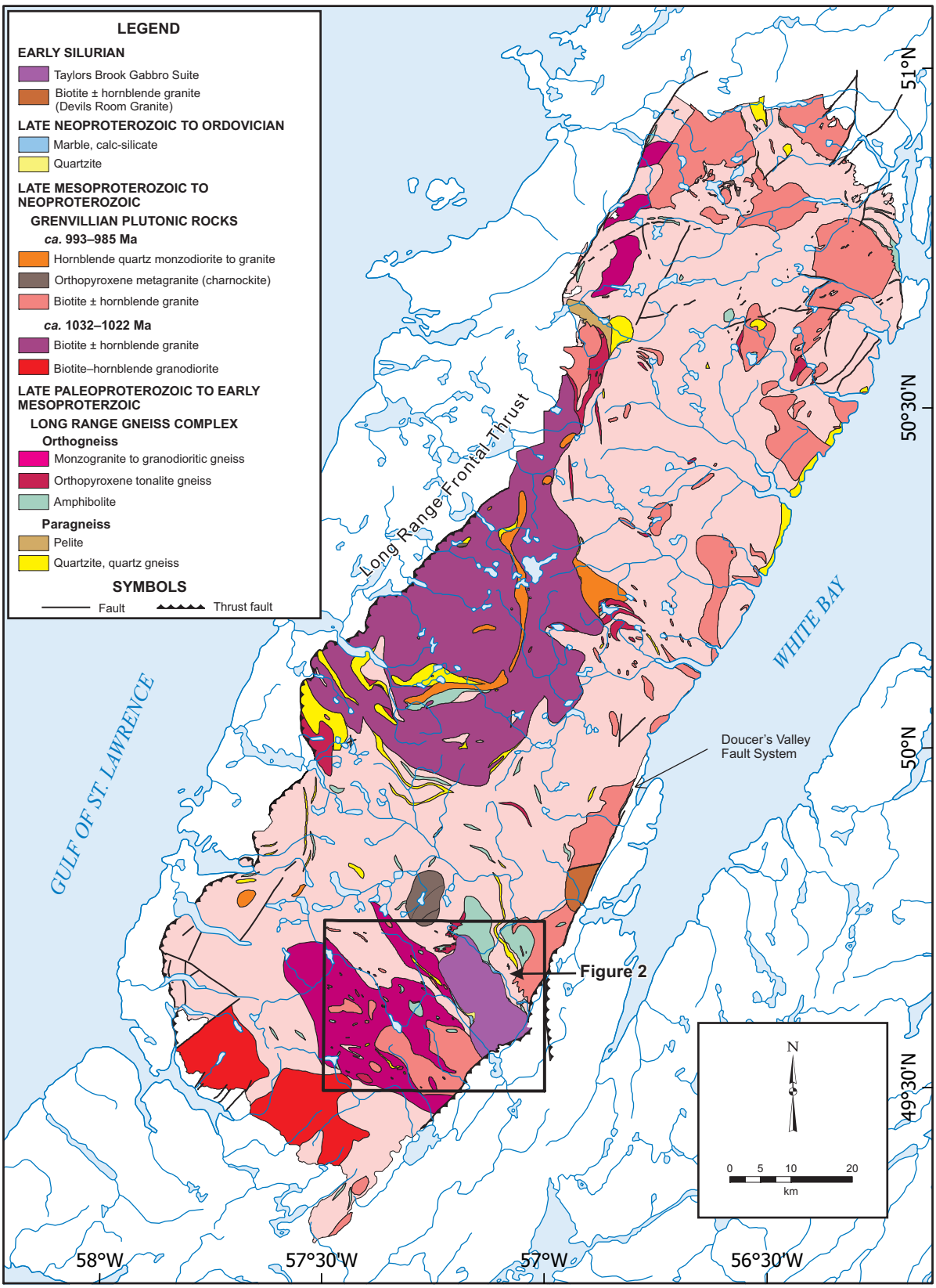

Figure 1. *Simplified geology of the Long Range Inlier. Modified from Hinchey (2010) and Owen (1991). The location of Figure 2 is outlined.*

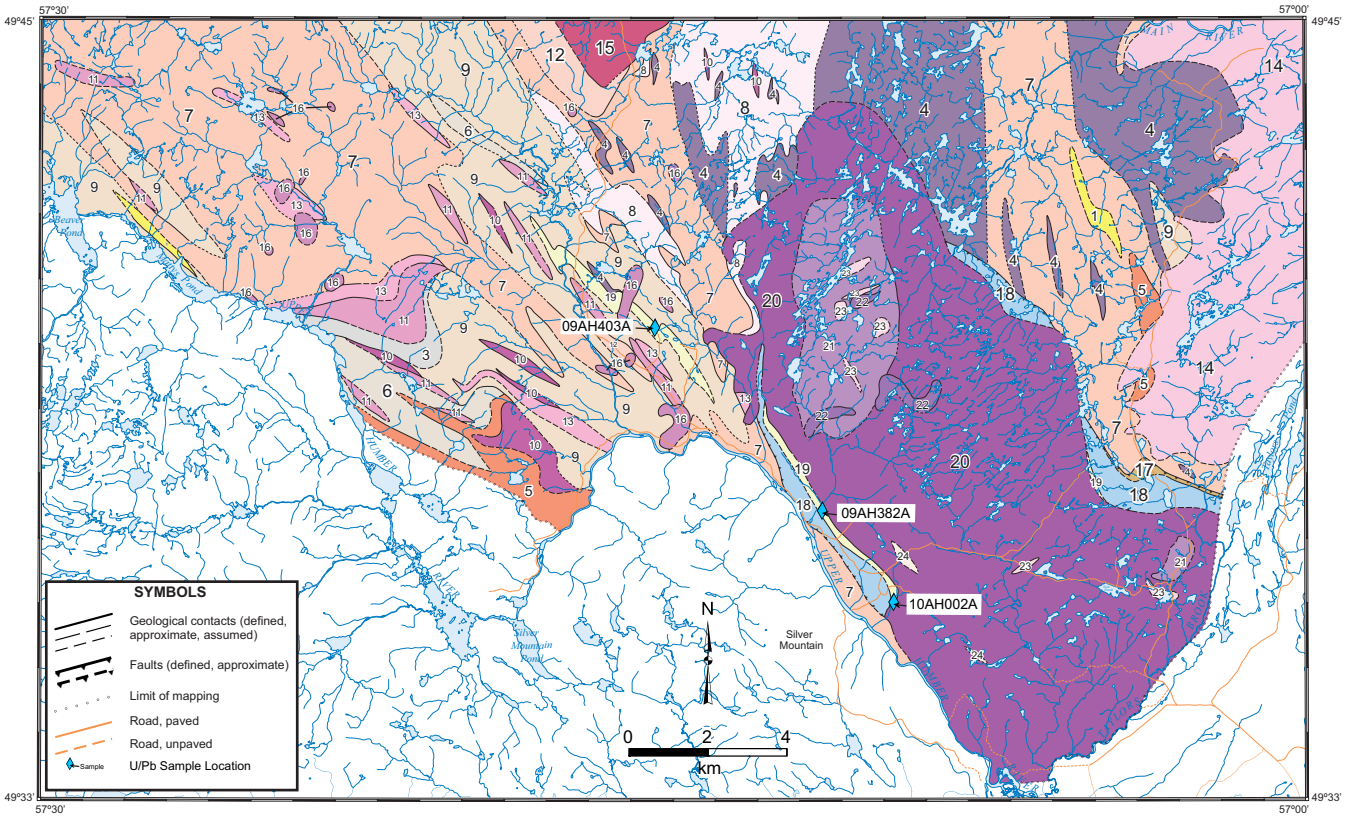

LEGEND

EARLY SILURIAN

- 24 Quartz–feldspar–porphyry dykes
- 23 Biotite monzogranite

Taylors Brook Gabbro Suite

- 22 Olivine gabbronorite to nortie
- 21 Pegmatitic gabbro to melanogabbro
- 20 Gabbro with minor leucogabbro, melanogabbro, and norite

LATE NEOPROTEROZOIC TO ORDOVICIAN

- 19 Semipelitic gneiss and quartzite
- 18 Marble to locally dolomite
- 17 Phyllite to pelitic schist

LATE MESOPROTEROZOIC TO NEOPROTEROZOIC

- 16 Hornblende metagabbro

GRENVILLIAN PLUTONIC ROCKS (~1056–970 Ma)

Potato Hill Pluton (~999 ± 4 Ma; Heaman *et al.*, 2002)

- 15 Coronitic orthopyroxene metagranite (charnockite)

Main River Pluton

- 14 Biotite ± hornblende monzogranite to quartz monzonite

Unnamed Intrusions

- 13 Biotite ± hornblende, potassium-feldspar augen metamonzogranite
- 12 Biotite metamonzogranite
- 11 Biotite ± hornblende metaquartz monzonite to metamonzogranite
- 10 Biotite–hornblende metagabbro

LATE PALEOPROTEROZOIC TO EARLY MESOPROTERZOIC

LONG RANGE GNEISS COMPLEX

Orthogneiss

- 9 Biotite hornblende ± orthopyroxene metagranodiorite to metadiorite
- 8 Orthopyroxene–biotite metatonalite to metagranodiorite
- 7 Biotite ± hornblende ± orthopyroxene monzogranitic to granodioritic gneiss
- 6 Biotite ± hornblende ± orthopyroxene monzogranite to quartz monzonite gneiss
- 5 Moderately foliated to locally gneissic metadiorite to metaquartz diorite
- 4 Amphibolite

Migmatites

- 3 Metatexite migmatite containing 15 to 20% leucosome

Paragneiss

- 2 Semipelitic to pelitic gneiss interlayered with psammitic gneiss
- 1 Interlayered quartzite and quartz-rich paragneiss

Figure 2. *Geology of the Silver Mountain map area. Modified after Hinchey (2020). Detrital zircon sample locations are plotted.*

GEOLOGY OF THE LONG RANGE INLIER

The Long Range Inlier of western Newfoundland is one of the largest exposures of Proterozoic crystalline basement rocks within the Appalachian orogen. It is not a simple stratigraphic inlier but rather represents a massif that was reactivated during the Appalachian orogeny. The approximately 8500 km^2 of basement rocks comprise the largest portion of the external Humber Zone. The Long Range Inlier forms a structural culmination that is bounded to the north, south and locally to the west, by Proterozoic to Paleozoic cover rocks. The western boundary is marked by a southeast-dipping thrust fault (the Long Range frontal thrust) that transported the Proterozoic crystalline rocks of the inlier onto autochthonous Cambro-Ordovician platformal strata and Taconic allochthonous rocks (Owen, 1991; Erdmer and Williams, 1995). Paleozoic overprinting of the inlier is marked by low-grade metamorphism and tectonic reworking along the Doucers Valley Fault system and emplacement of post-deformational intrusions, *e.g.*, Devils Room granite and Taylor Brook Gabbro Suite (TBGS; Figures 1 and 2). The Doucers Valley Fault system is an imbrication of the Long Range–Cabot Fault system. These fault systems mark wide tectonic zones of anastomosing ductile and brittle-ductile shear zones that are crosscut and over-printed by intense high-level brittle-ductile and brittle structures, largely obliterating earlier ductile deformation structures. These faults are long-lived, complex, crustal-scale features that initiated as rifts during the Ediacaran opening of the Taconic Seaway and were reactivated throughout the late Paleozoic assembly of the supercontinent Pangea (Lock, 1969; Smyth and Schillereff, 1982; Hyde *et al.*, 2007; Sandeman *et al.*, 2024). Their periodic reactivation controlled deformation styles during the Appalachian orogen and later lateral, orogen-parallel transport of accreted microcontinents and terranes (Waldron *et al.*, 2015; van Staal *et al.*, 2021), as well as the generation and evolution of Carboniferous sedimentary basins in the region (Hyde *et al.*, 2007; Hinchey *et al.*, 2022).

The Long Range Inlier is composed largely of amphibolite- to granulite-facies orthogneiss with minor paragneiss (Figure 2). The geology is broadly divisible into the following tectonic divisions: 1) High-grade, Long Range Gneiss Complex, dominantly orthogneiss with lesser paragneiss (in part Sequence B); 2) Weakly to strongly foliated plutonic rocks; interpreted to be Grenvillian; 3) Mafic dykes (Long Range dyke swarm); 4) Thin remnants of latest Neoproterozoic to Paleozoic cover sequence (includes Sequence A), and 5) Early Silurian gabbro intrusions and minor felsic intrusions with volcanic equivalents.

PETROGRAPHY AND U–Pb GEOCHRONOLOGY

ANALYTICAL METHODS

Zircon separates were extracted using standard crushing techniques, and heavy mineral concentrates were produced using a Wilfley™ table, heavy liquids and a Frantz™ isodynamic separator before hand-picking in ethanol under a binocular microscope. Subdivision of zircon populations was initially carried out using a binocular microscope and standard optical criteria (*i.e.*, colour, morphology and inclusion characteristics). A subset (average of n = 20–30 per population) of grains selected from each zircon population identified using optical criteria were isolated, photographed in transmitted light and subsequently mounted in epoxy resin and polished to expose grain cores. Grain mounts were then carbon coated and imaged using backscattered electron (BSE) and cathodoluminescence (CL) image analysis. Analysis targeted clear, inclusion-free locations that were interpreted to represent single age domains.

U/Pb and Pb/Pb isotopic ratios of the unknown samples and zircon standards analyzed for data quality control purposes were measured using a Finnigan ELEMENT XR double focusing magnetic sector field ICP-MS coupled to Geolas 193nm excimer laser located in the Inco Innovation Centre, Memorial University of Newfoundland. Zircon grains previously imaged by BSE to detect internal zoning were ablated using a 10 µm laser beam rastered over the sample surface to create a 40 x 40 µm square spot. Only one spot per grain was analyzed. Laser energy was set at 5 J/cm^2 with a repetition rate of 10 Hz. The sample introduction system enabled simultaneous nebulization of an internal standard tracer solution and laser ablation of the solid sample. The tracer solution, consisting of a mixture of natural Tl (^{205}Tl/^{203}Tl = 2.3871) and enriched ^{233}U, ^{209}Bi and ^{237}Np (concentrations of *ca.* 1 ppb per isotope) transported in a mixed Ar-He carrier gas, was employed to correct for instrumental mass bias. Time-resolved data acquisitions (120–180 s experiments) consisted of *ca.* 20–30 s measurement of the Ar-He gas blank and aspirated tracer solution prior to introduction of ablated material. Data were collected on unknown zircon samples and two zircon standards, PL (337 Ma) and 91500 (*ca.* 1065 Ma), for which U–Pb and Pb–Pb ages had been previously determined by ID TIMS. Typically, 10–14 analyses of unknowns were collected for every 6 analyses of the standards. Analyzing and treating the zircon standards as unknowns is a robust quality control procedure that allows assessment of the accuracy and precision of the technique during an analytical session. This approach ensures the efficiency of the mass-bias correction as well as

the correction for laser-induced fractionation. During ablation, U and Pb isotopes and tracer solution signals were acquired in time-resolved peak-jumping, pulse-counting mode with one point measured per peak. The range of masses measured for each analysis was: ^{202}(Hg) (flyback or settling mass), ^{204}(Hg), ^{203}(Tl), ^{205}(Tl), ^{206}(Pb), ^{207}(Pb), ^{209}(Bi), ^{232}(Th), ^{233}(U), ^{237}(Np), ^{238}(U). Three oxide masses ^{249}(^{233}U^{16}O), ^{253}(^{237}Np^{16}O) and ^{254}(^{238}U^{16}O) were measured to correct for oxide formation by adding signal intensities at masses 249, 253 and 254 to the intensities at masses 233, 237 and 238, respectively. Raw data were corrected for the electron multiplier's dead time (20 ns) and processed offline in an Excel spreadsheet-based program (Lamdate; Košler *et al.*, 2002). For a detailed technique description, *see* Košler *et al.* (2002) and Cox *et al.* (2003). Data reduction included correction for gas blank, laser-induced elemental fractionation of Pb and U *via* the intercept method after Sylvester and Ghaderi (1997), and instrument mass bias. The mass-bias correction utilized the power law and the ratio measurements of the isotopic tracer solution (Horn *et al.*, 2000; Košler *et al.*, 2002). Th and U concentrations for the zircons were calibrated with zircon 91500. Isoplot v. 2.06 (Ludwig, 2003), in conjunction with the LAMdate Excel spreadsheet program, was used to calculate U–Pb ages of unknowns and plot data (Košler *et al.*, 2002).

Concordant values were calculated using the ratio of ^{206}Pb/^{238}U and ^{207}Pb/^{206}Pb; analyses with excessive discordance (>10% discordant, >5% reversely discordant) were excluded from plots and interpretations. For analyses with ^{207}Pb/^{206}Pb and ^{206}Pb/^{238}U dates that are older than ~1.2 Ga, age interpretations are based on ^{207}Pb/^{206}Pb dates; otherwise, age interpretations are based on ^{206}Pb/^{238}U dates (Gehrels *et al.*, 2008) (Supplemental Material S1). Ages are reported at 1σ uncertainty and presented in Kernel density estimate (KDE) plots created in R (Figures 3–5).

U–Pb GEOCHRONOLOGY

METASEDIMENTARY SEQUENCE A: PSAMMITE (09AH382A)

This sample was collected from metasedimentary Sequence A on the west side of the TBGS (Figure 2). The sample is a foliated, thin-layered, brown-weathering, biotite–muscovite–garnet psammite (Plate 1A, B). The psammite is interlayered with quartz-rich layers. In thin section, the psammite's primary minerals are quartz and plagioclase (Plate 1C, D). Accessory phases include garnet, muscovite, biotite and cordierite (*see* also Plate 4A). Garnet grains are fractured and appear to be replaced by potassium feldspar, biotite, epidote and chlorite.

The detrital population has zircon grains that are mostly subrounded to rounded with aspect ratios of 2:1 or 1:1. There is a minor population of elongate grains with aspect ratios of 4:1. Most grains are clear of inclusions and are homogeneous in appearance (Figure 3D). In BSE imagery, the grains are characterized by weakly developed sector zoning. Of 109 zircon analyses, sample 09AH382A yielded 49 individual dates from different grains that passed the discordance filter. These dates consist of 12% Archean (3200–2500 Ma), 14% Paleoproterozoic (2500–1600 Ma), 31% Mesoproterozoic (1500–1300 Ma), 28% Grenvillian (1090–980 Ma), 8% Post-Grenvillian (975–920 Ma) and 6% ≤920 Ma analyses. The three youngest grains (≤920 Ma) were dated at 909 ± 20 Ma, 809 ± 19 Ma and 551 ± 12 Ma. The sample shows a polymodal distribution with a dominant peak at 1110 Ma and subordinate peaks at 1000, 1300, 1800 and 2700 Ma. The maximum depositional age calculated using the maximum likelihood age (MLA) algorithm (Vermeesch, 2023) at 1σ for this sample is 554 ± 15 Ma (Figure 3C).

METASEDIMENTARY SEQUENCE A: PSAMMITE (10AH002A)

This sample, collected from the same mapped metasedimentary sequence as sample 09AH382A, was located along strike to the southeast (Figure 2). The sample is a foliated, thin-layered, grey-weathering psammite (Plate 2A, B). It is interlayered with quartzite layers at the cm scale. Beds are laterally discontinuous and 1–5 cm thick. The psammite consists of potassium feldspar and biotite with lesser plagioclase (Plate 2C, D). Accessory phases include muscovite, corundum and tourmaline (*see* also Plate 4B). Oxides include rutile and hercynite. Minor pyrite and pyrrhotite also occur.

The zircon grains in sample 10AH002A are mostly subrounded to rounded with aspect ratios of 2:1 or 1:1 (Figure 4D). A small population of grains are broken and angular, with aspect ratios of 3:1. In BSE imagery, the grains are characterized by weakly developed sector zoning. Of 111 zircon analyses, sample 10AH002A yielded 30 individual zircon dates that passed the discordance filter, which consist of 20% Archean (3500–2500 Ma), 47% Paleoproterozoic (2500–1600 Ma), 27% Mesoproterozoic (1600–1200 Ma) and 7% Grenvillian (1090–980 Ma) analyses. The samples show a polymodal distribution with a dominant peak at 1800 Ma and subordinate peaks at 1200, 1900 and 2700 Ma. The maximum depositional age calculated using the MLA algorithm at 1σ for this sample is 996 ± 26 Ma (Figure 4C).

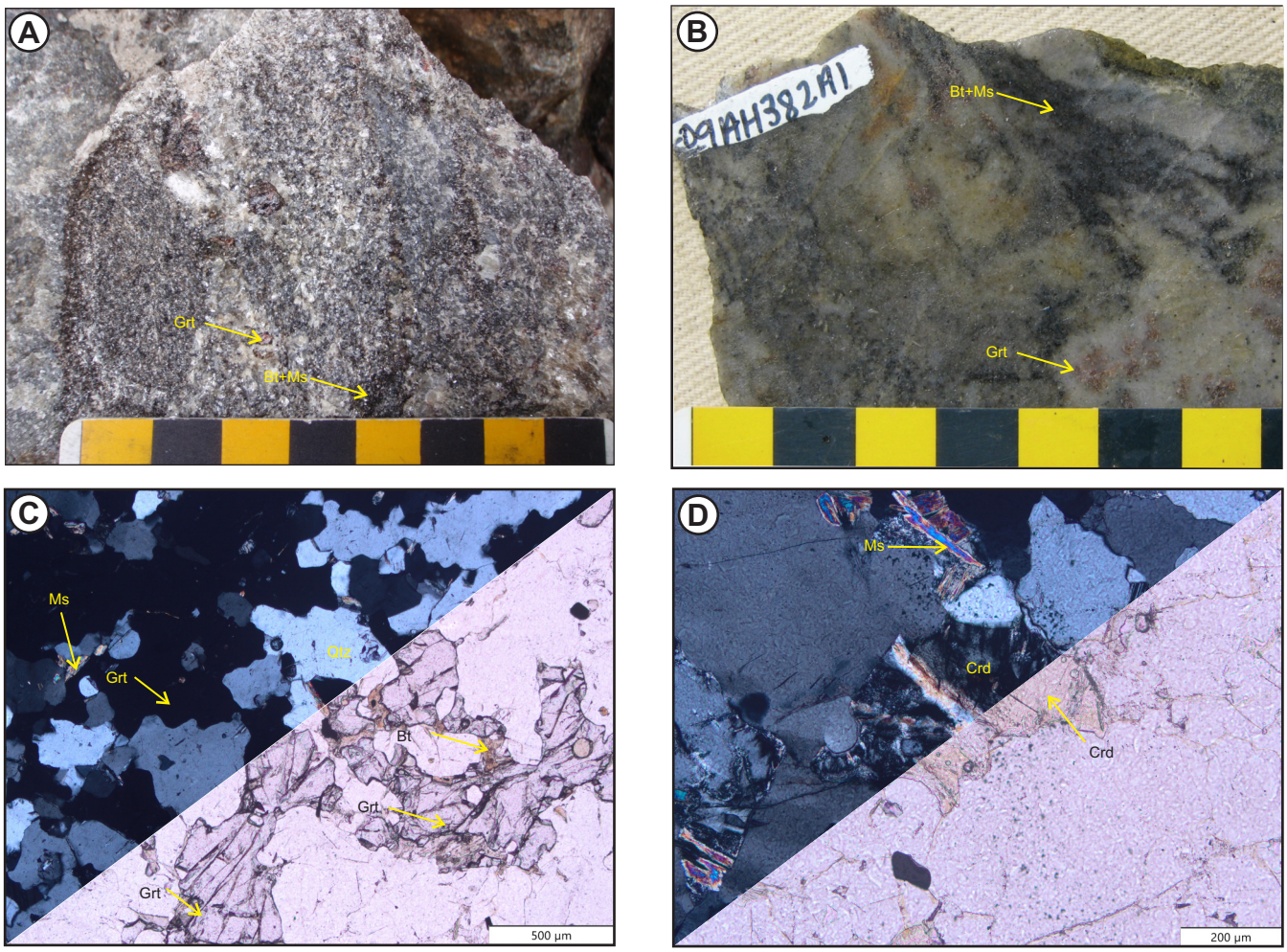

Plate 1. *Representative images of U–Pb geochronology sample 09AH382A. A) Field photograph; B) Scan of rock slab. Photomicrographs in C (plane-polarized light) and D (cross-polarized light). All mineral abbreviations are from Whitney and Evans (2010).*

METASEDIMENTARY SEQUENCE B: SEMIPELITE (09AH403A)

This sample was collected from a metasedimentary sequence located 3 km to the west of the TBGS (Figure 2). The metasedimentary sequence is infolded with orthogneiss of the Long Range Gneiss Complex and was thought to represent some of the oldest rocks in the area. The sample is a foliated, thin-layered, brown-weathering, muscovite–garnet–biotite semipelite (Plate 3A, B). It is interlayered with psammitic layers at the cm scale. Garnet forms subhedral porphyroblasts that range in width from 1 to 5 mm. The semipelite mostly consists of plagioclase, quartz and biotite (Plate 3C, D). Accessory phases include muscovite, rutile and zircon (Plate 4C). Disseminated pyrite occurs throughout.

Zircon grains in this sample are mostly subrounded to rounded with aspect ratios of 2:1 or 1:1 (Figure 5D). A small population of elongate grains have aspect ratios of 4:1. In BSE imagery, the grains are characterized by weakly developed oscillatory zoning. Some grains have uranium rich cores. From 100 individual zircon analyses, sample 09AH382A yielded 46 dates that passed the discordance filter. These dates consist of 24% Mesoproterozoic (1500–1300 Ma), 26% Grenvillian (1090–980 Ma), 44% Post-Grenvillian (975–950 Ma) and 7% <900 Ma analyses. The samples show a polymodal distribution with a dominant peak at 920 Ma and subordinate peaks at 970 Ma and 1400 Ma. The maximum depositional age calculated using the MLA algorithm at 1σ for this sample is 906 ± 7 Ma (Figure 5C).

DISCUSSION

The geochronological constraints presented above suggest that there are variable detrital sources preserved in the metasedimentary sequences in the Long Range Inlier. One

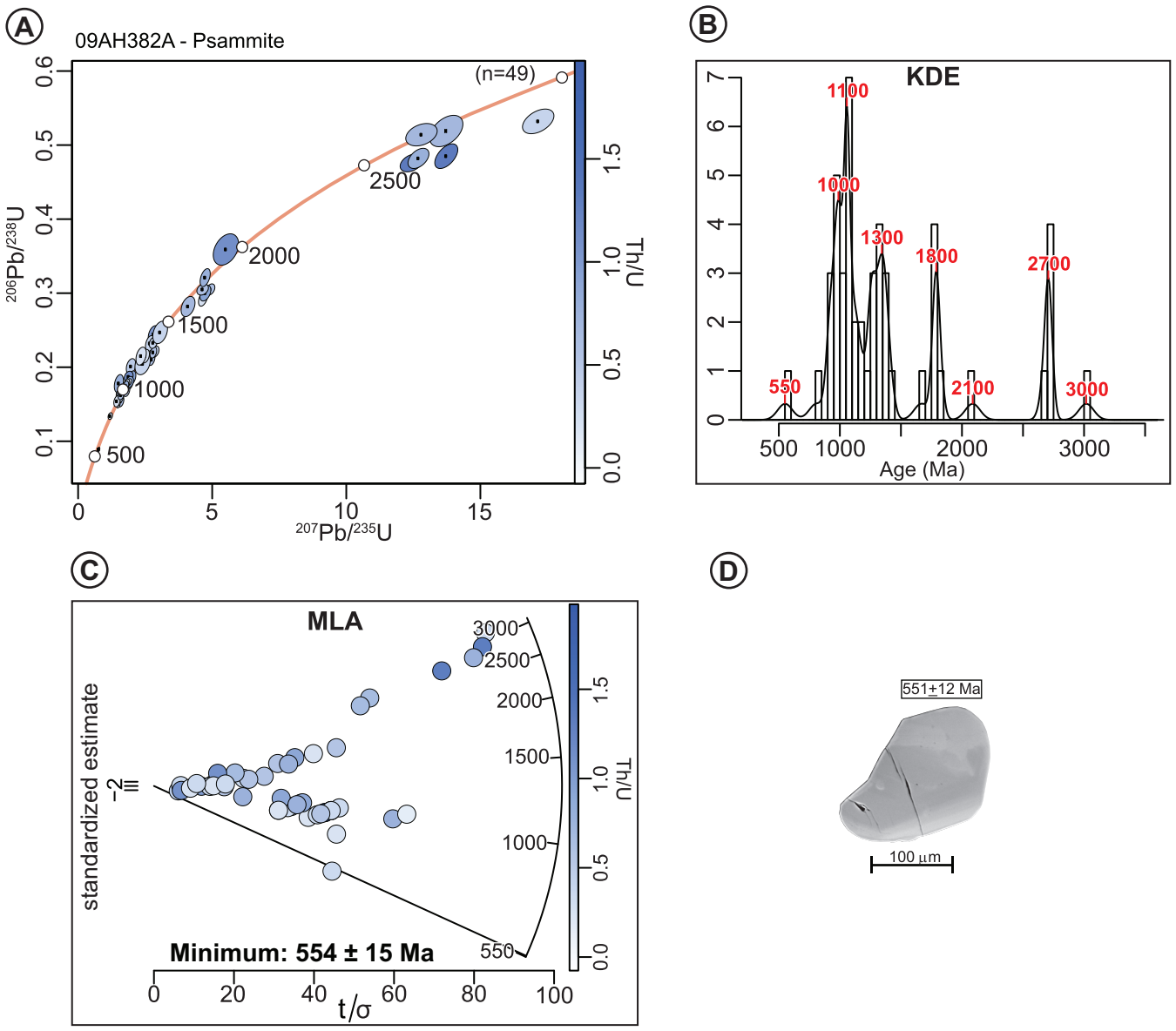

Figure 3. *A–C: U–Pb geochronological data for detrital zircon analyses that passed the relative age discordance filter (<10% discordant and <5% reversely discordant) for psammite sample 09AH382A from metasedimentary Sequence A. A) Wetherill concordia diagram, with error ellipses shown at 68.3% confidence; B) Kernel density estimate (KDE) plot with age peaks indicated in red text (in Ma); C) Radial plot and maximum depositional age estimate at 1s error following the maximum likelihood age (MLA) method of Vermeesch (2023); D) Representative BSE image of a zircon grain from sample 09AH382A. Analytical data is presented in Supplemental Material S1.*

sample from metasedimentary Sequence A that flanks the TBGS had a maximum depositional age of 554 ± 15 Ma. This supports the field-based hypothesis of Hinchey (2010) that the sequence is likely Cambro-Ordovician and is probably part of the Labrador and Port au Port groups based on lithological similarities (Figure 6). These groups may have been para-autochthonous. The detrital zircon signatures indicate a large role for Grenvillian detritus in sample 09AH382A. The second sample from Sequence A yields a maximum depositional age of 996 ± 26 Ma and contains a large amount of Paleoproterozoic detritus. Both samples have a minor contribution of Archean detritus. The range of maximum depositional ages can be interpreted in two ways: 1) The two samples from Sequence A may represent different stratigraphic levels that were fed by local sources of different ages that varied over time; 2) Alternatively, the mapping at 1:50 000 scale, which interpreted the outcrops as part of the same unit may be incorrect and thus, the two outcrops

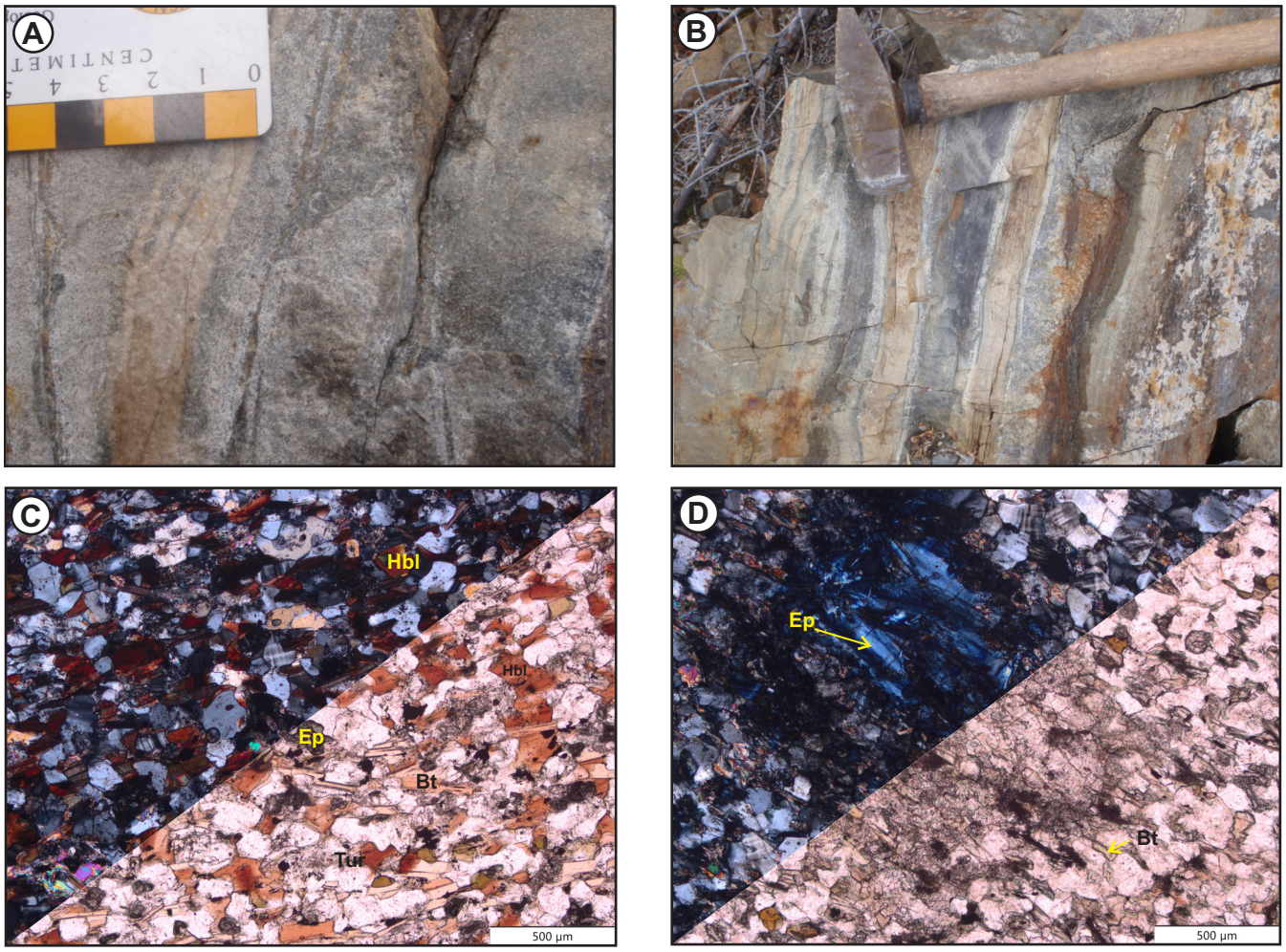

Plate 2. *Representative images of U–Pb geochronology sample 10AH002A. A, B) Field photographs of the outcrop from which the sample was collected. Hammer in B is 48 cm long. Photomicrographs in C (plane-polarized light) and D (cross-polarized light). All mineral abbreviations are from Whitney and Evans (2010).*

may represent two distinct sequences with different depositional histories.

A lack of young, post-Grenvillian-aged zircon grains in rocks from both the allochthonous and autochthonous cover sequences of the Laurentian margin is not uncommon. Samples from the base of the autochthonous Bradore Formation (Labrador Group; Figure 6) yielded detrital zircon dates between 1223 ± 35 and 930 ± 23 Ma (Cawood and Nemchin, 2001); and detrital zircon dates from a second Bradore Formation sample near White Bay ranged from 1523 ± 4.2 Ma to 988 ± 3.9 Ma (Allen, 2009). Similarly, samples from the base of the allochthonous Summerside Formation (Curling Group) yielded zircon ages that largely ranged from 1132 ± 22 to 999 ± 12 Ma, with two younger grains with ages of 586 ± 12 and 628 ± 11 Ma (Cawood and Nemchin, 2001). Similar detrital age profiles for the same formation were reported by Allen (2009), with ages ranging from 1521 ± 5.5 to 980 Ma and two younger grains at 582 ± 9 and 612 ± 10 Ma. At even higher stratigraphic levels in the Foreland succession, the Clam Bank and Red Island Road formations preserve only minor to no contributions of post-Grenvillian detritus (*see* White *et al.*, 2019). Therefore, the lack of post-Grenvillian zircon grains in the second sample (10AH002A) from Sequence A does not preclude it from having a Cambro-Ordovician depositional age. If the two samples from Sequence A are part of the same geological unit, as indicated by the bedrock mapping, then the contrasting detrital signatures between the samples suggest the presence of localized, isolated depositional basins. This implies that the depositional environment was strongly influenced by the proximity and characteristics of the source material supplying sediment to these basins, rather than reflecting a more regional-scale depositional system.

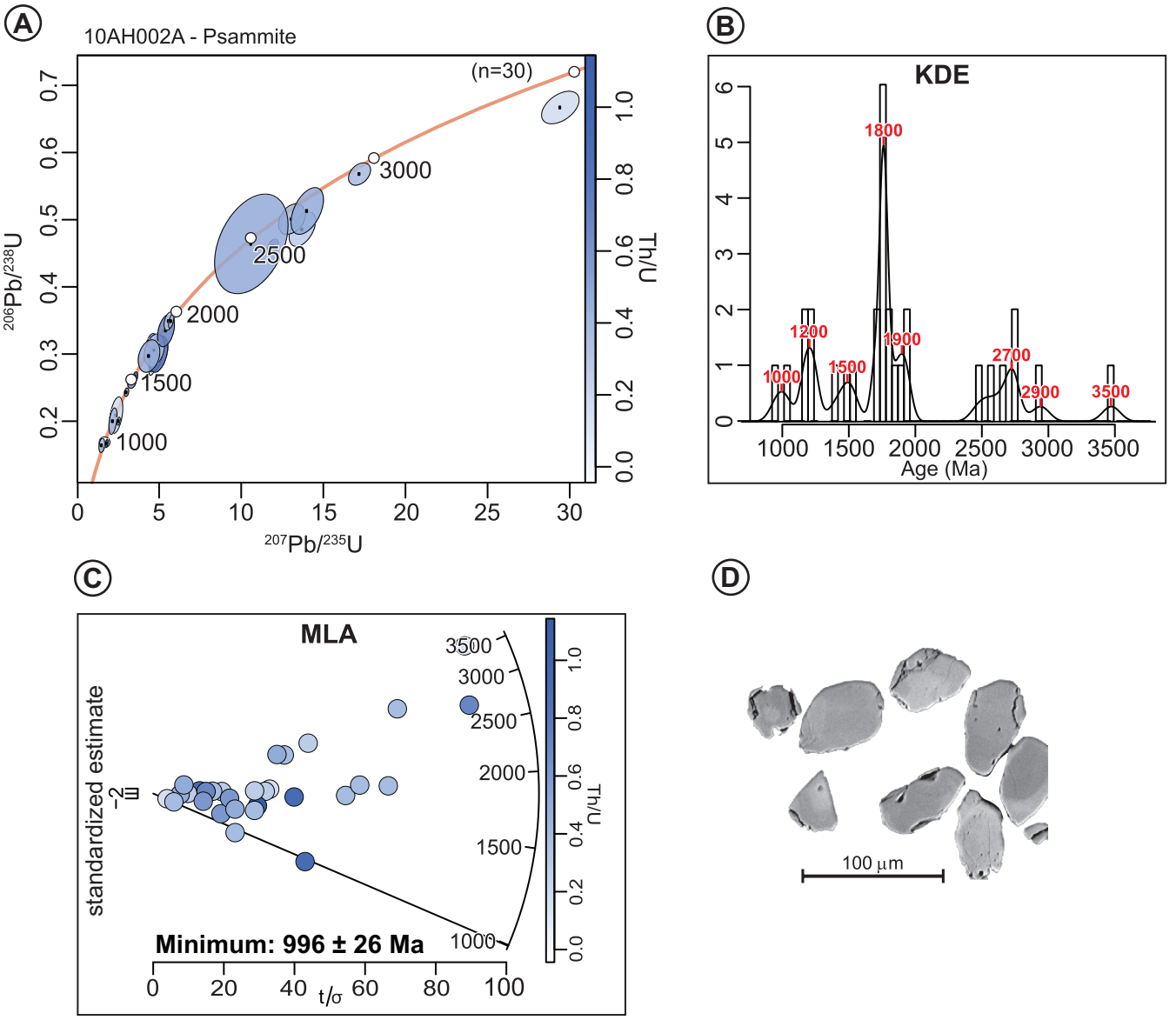

Figure 4. *A–C: U–Pb geochronological data for detrital zircon analyses that passed the relative age discordance filter (<10% discordant and <5% reversely discordant) for psammite sample 10AH002A from metasedimentary Sequence A. A) Wetherill concordia diagram, with error ellipses shown at 68.3% confidence; B) Kernel density estimate (KDE) plot with age peaks indicated in red text (in Ma); C) Radial plot and maximum depositional age estimate at 1s error following the maximum likelihood age (MLA) method of Vermeesch (2023); D) Representative BSE images of zircon grains from sample 10AH002A. Analytical data is presented in Supplemental Material S1.*

The maximum depositional age for the metasedimentary Sequence B is 906 ±7 Ma, which is far younger than the previous mapping indicated (Owen, 1991; Hinchey, 2020). The age is younger than the youngest Grenvillian orogenic event, the Rigolet orogen (1010–980 Ma), which was marked by low-pressure metamorphism and plutonism (Rivers and Murphy, 2012). The post-Grenvillian (*ca.* 985–920 Ma) period (Gower, 2019) corresponds to a magmatic event in the exterior thrust belt of the Grenville orogeny and waning tectonothermal activity recorded in U–Pb ages from rutile grains in Labrador. The detrital signature of Sequence B indicates either: i) A post-Grenvillian rifting event that would have created a basin at *ca.* 900 Ma, where sediments from eroding Grenvillian and post-Grenvillian rocks were deposited perhaps related to the prolonged opening of the Asgard sea; or ii) Sequence B is also part of the Laurentian cover sequence. Further study is required to differentiate between these two possibilities.

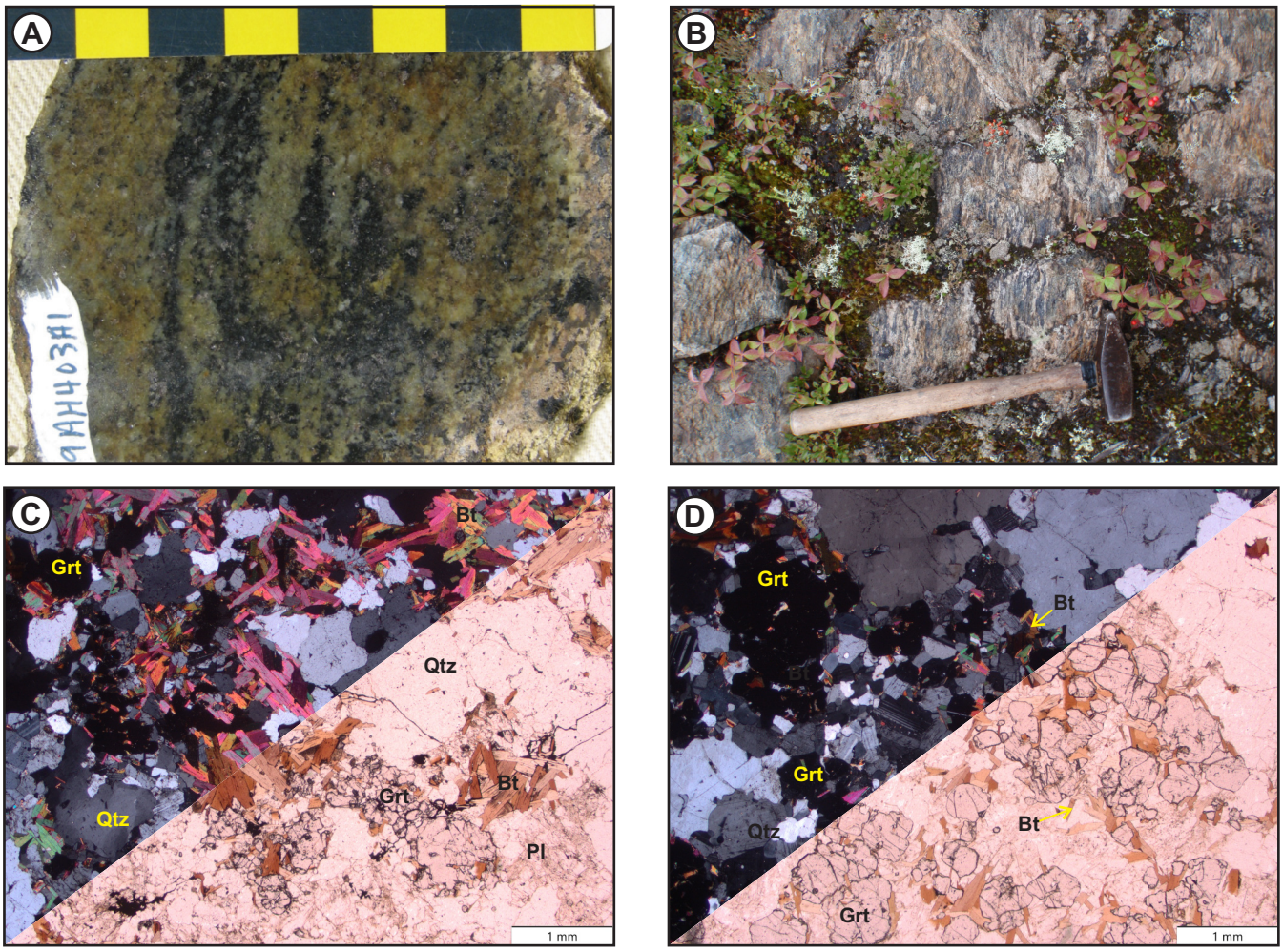

Plate 3. *Representative images of U–Pb geochronology sample 09AH403A. A) Scan of rock slab; B) Field photograph. Hammer is 48 cm long. Photomicrographs in C (plane-polarized light) and D (cross-polarized light). All mineral abbreviations are from Whitney and Evans (2010).*

These detrital signatures indicate that the depositional history of the Long Range Inlier metasedimentary rocks is more complex than previously recognized. The maximum depositional ages of all three samples range over 400 m.y., similar to the detrital signatures preserved within the Laurentian cover sequence elsewhere (Cawood and Nemchin, 2001; Allen, 2009; White *et al.*, 2019). Sequence A is likely part of the Cambro-Ordovician Laurentian cover sequence that was deposited onto the Long Range Inlier (Figure 7). The antiquity of Sequence B remains unclear; however, the post-Grenvillian orogenic age indicates that the geological interpretation and bedrock mapping of the metasedimentary units by Hinchey (2010, 2020) need refining. This also raises questions about the provenance of the other metasedimentary sequences that are mapped as part of the Long Range Gneiss Complex (*see* Figures 1 and 2). Further detrital geochronological studies are required to improve our understanding of the history of the Long Range Inlier and associated/proximal metasedimentary rocks.

CONCLUSION

New U–Pb geochronological data derived from detrital zircon analysis of metasedimentary sequences in the Long Range Inlier reveals a more complex evolutionary history than previously understood. Two psammite samples from Sequence A yielded maximum depositional ages (calculated using the maximum likelihood age algorithm at 1σ) of 554 ± 15 and 996 ± 26 Ma, suggesting that this sequence is likely Cambro-Ordovician in age and may correlate with parts of the Labrador and Port au Port groups. The absence of Neoproterozoic or younger zircon in one of the samples is consistent with other detrital signatures observed in Laurentian cover sequence rocks. Sequence A is likely

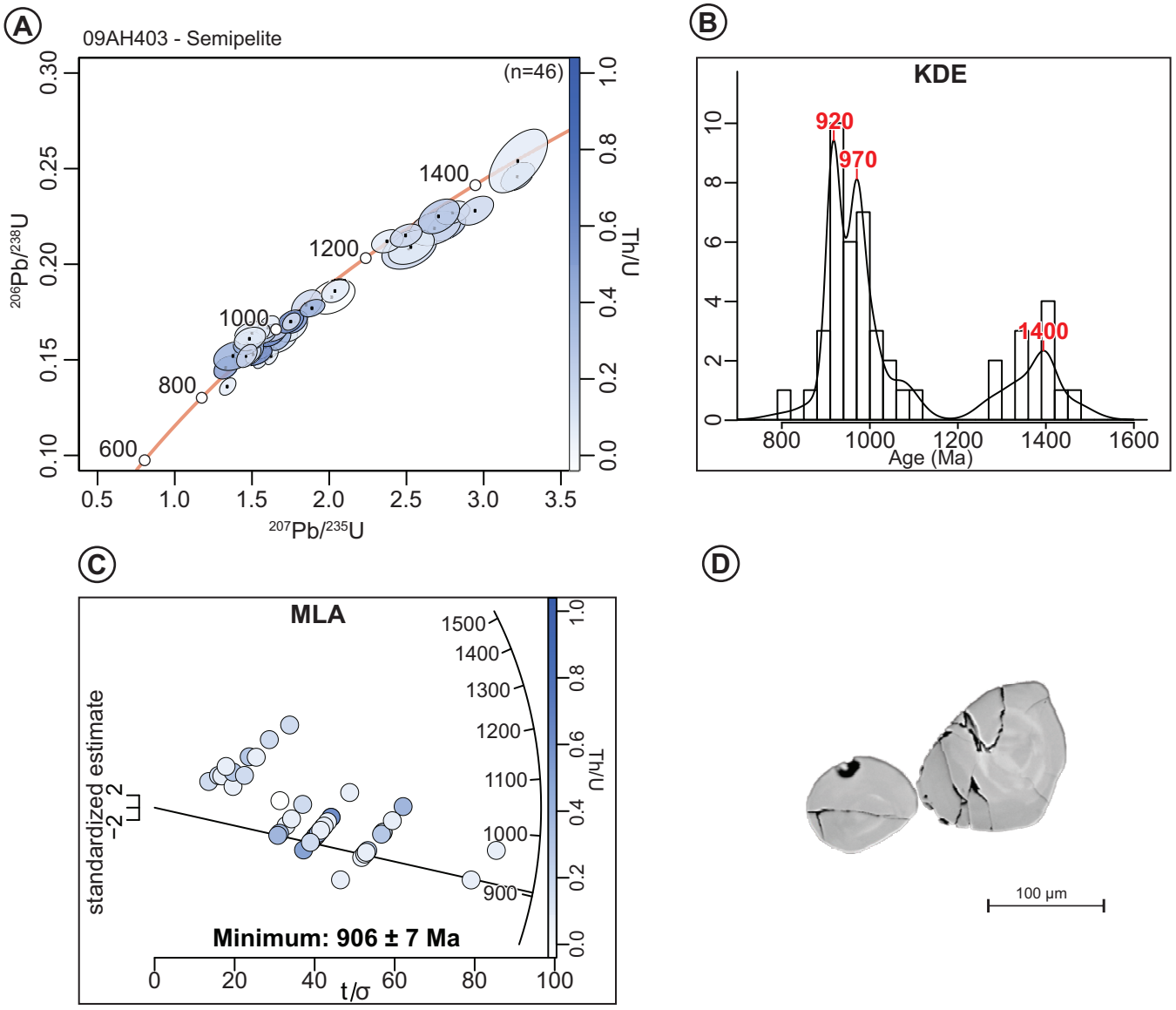

Figure 5. *A–C: U–Pb geochronological data for detrital zircon analyses that passed the relative age discordance filter (<10% discordant and <5% reversely discordant) for semipelite sample 09AH403A from metasedimentary Sequence B. A) Wetherill concordia diagram, with error ellipses shown at 68.3% confidence; B) Kernel density estimate (KDE) plot with age peaks indicated in red text (in Ma); C) Radial plot and maximum depositional age estimate at 1s error following the maximum likelihood age (MLA) method of Vermeesch (2023); D) Representative BSE images of zircon grains from sample 09AH403A. Analytical data is presented in Supplemental Material S1.*

autochthonous (para?) and was metamorphosed during the intrusion of the TBGS. The detrital zircon signatures indicate varying ages of detritus between the two samples, one being heavily influenced by Grenvillian detritus (*ca.* 1000–1300 Ma), while the other was dominantly influenced by Paleoproterozoic (*ca.* 1800 Ma) detritus. The contrasting signatures suggest the presence of localized, isolated depositional basins that were primarily affected by proximal source material.

The maximum depositional age of 906 ± 7 Ma for the metasedimentary Sequence B is notably younger than previous mapping-based interpretations. It is also younger than the youngest Grenvillian orogenic phase (the Rigolet orogen; 1010–980 Ma) and the post-Grenvillian period (*ca.* 985–920 Ma). The detrital signature of Sequence B suggests either a post-Grenvillian rifting event, creating a basin ca. 900 Ma, perhaps related to the opening of the Asgard Sea, or that Sequence B is also part of the Laurentian cover sequence. This finding necessitates a re-evaluation of the

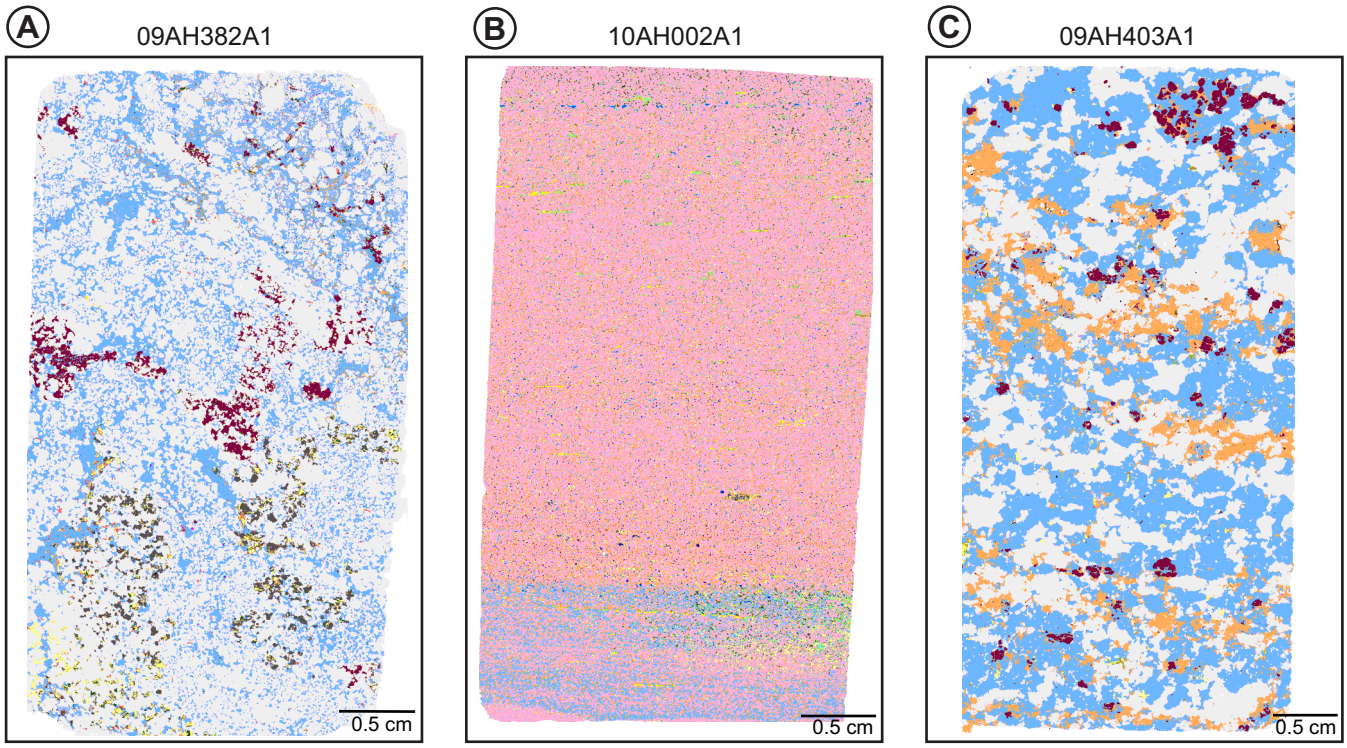

Weight Percentage(%) Samples	09AH382A1	10AH002A1	09AH403A1
Quartz	66.68	0.06	39.26
Plagioclase	22.40	8.15	40.69
Biotite	1.44	20.31	14.40
K Feldspar	0.12	58.38	0.10
Muscovite	1.50	6.47	0.53
Garnet	3.96	-	4.47
Cordierite	1.97	-	-
Orthopyroxene	-	0.01	-
Chlorite	0.88	1.40	0.01
Calcite	0.70	-	-
Epidote	-	2.18	-
Tourmaline	-	0.42	-
Hercynite	-	0.71	-
Corundum	-	0.82	-
Aluminum silicate	-	0.11	-
Rutile	0.05	0.02	0.15
Rutile-Ilm mix	0.10	-	0.03
Titanite	0.02	0.19	-
Apatite	0.06	0.05	-
Zircon	0.06	0.02	0.05
Monazite	0.01	0.02	-
Iron Oxide	0.01	-	0.01
Pyrite	-	0.04	0.22
Ilmenite	0.70	-	0.01
Pyrrhotite	0.01	0.62	0.05
Chalcopyrite	-	0.01	-

Plate 4. *Mineral Liberation Analysis-Scanning Electron Microscopy images of thin-sections from the U–Pb geochronology samples. A) 09AH382A; B) 10AH002A; C) 09AH403A.*

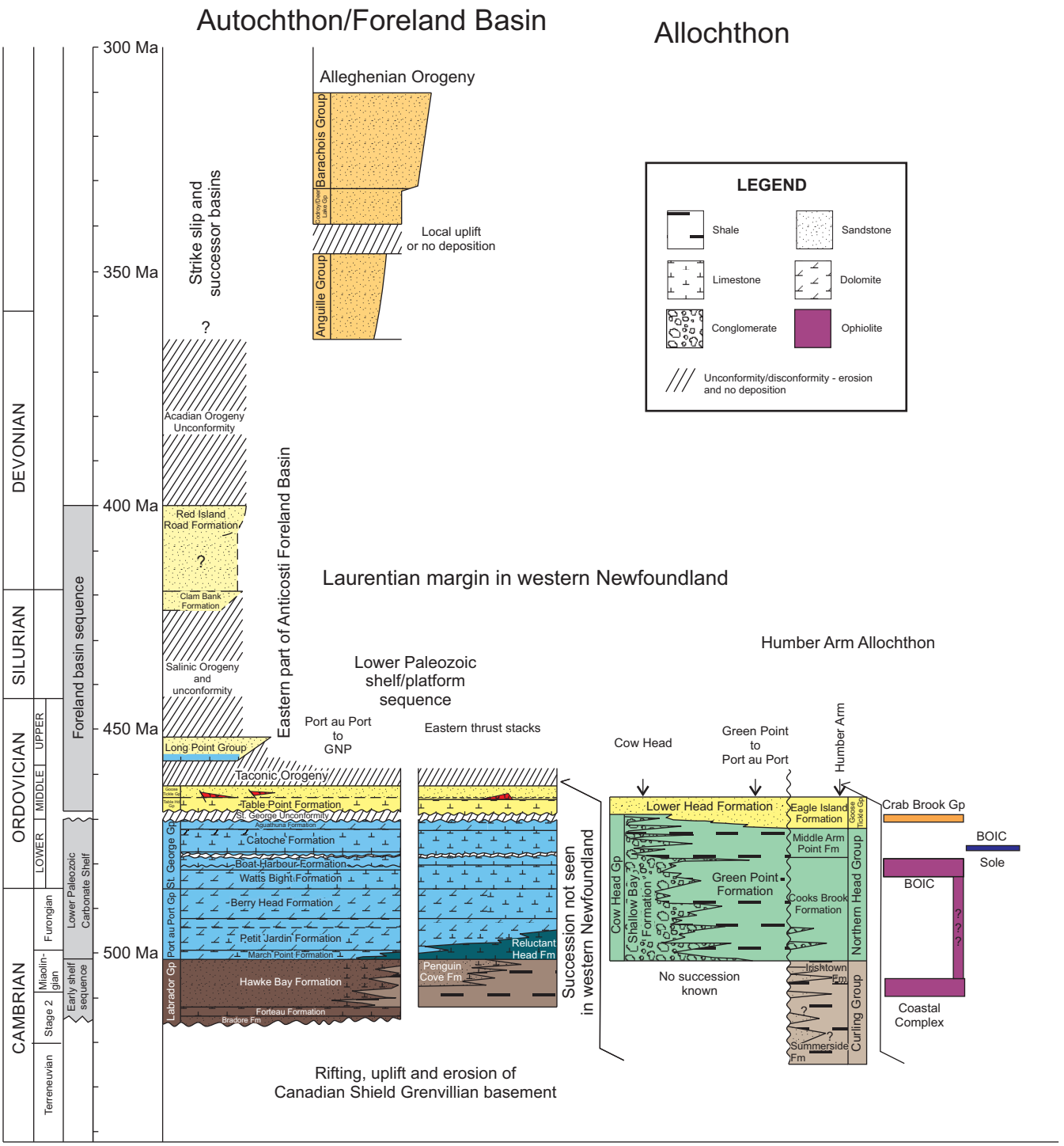

Figure 6. *Simplified stratigraphy of lower Paleozoic sequences in western Newfoundland modified after Hinchey* et al. *(2023). BOIC–Bay of Islands Ophiolite Complex.*

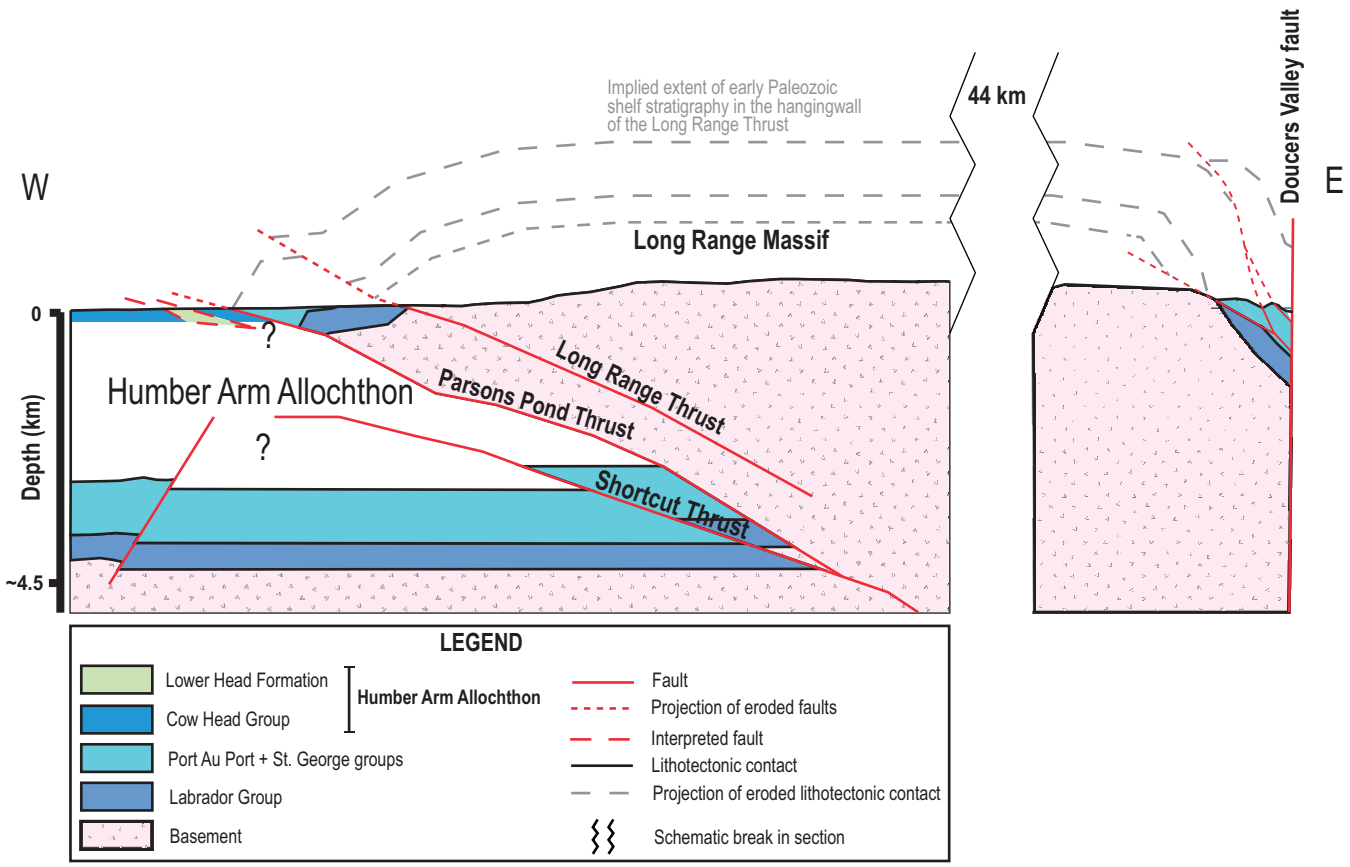

Figure 7. *Illustration of the location of Laurentian cover sequence over the Long Range Inlier. Modified after Allen (2009).*

tectonic history of the region, as it contradicts earlier assumptions regarding the age of these sequences and their geological context. This study underscores the importance of detrital zircon geochronology in unravelling the complex geological history of the Long Range Inlier. Future research should focus on additional geochronological investigations and detailed structural and lithological analyses to refine our understanding of the depositional environments and tectonic processes that have shaped this region within the broader context of the Appalachian orogen.

ACKNOWLEDGMENTS

The manuscript was improved by the helpful reviews of John Hinchey. Kim Morgan and Evie Li are thanked for their cartographic support.

REFERENCES

Allen, J.S.
2009: Paleogeographic reconstruction of the St. Lawrence promontory, western Newfoundland. University of Kentucky, Doctoral Dissertations, Lexington, Kentucky. https://uknowledge.uky.edu/gradschool_diss/732

Barbero, E., Delavari, M., Dolati, A., Vahedi, L., Langone, A., Marroni, M., Pandolfi, L., Zaccarini, F. and Saccani, E.
2020: Early Cretaceous plume–ridge interaction recorded in the Band-e-Zeyarat Ophiolite (North Makran, Iran): New constraints from petrological, mineral chemistry, and geochronological data. Minerals, Volume 10.2020, Issue 12, Article 1100, 36 pages. https://doi.org/10.3390/min10121100

Cawood, P.A. and Nemchin, A.A.
2001: Paleogeographic development of the east Laurentian margin: Constraints from U-Pb dating of detrital zircons in the Newfoundland Appalachians. Geological Society of America, Bulletin 113(9), pages 1234-1246. https://doi.org/10.1130/0016-7606(2001)113<1234:Pdotel>2.0.Co;2

Cox, R.A., Wilton, D.H.C. and Košler, J.
2003: Laser-ablation U-Th-Pb in situ dating of zircon and allanite: An example from the October Harbour

granite, central coastal Labrador, Canada. Canadian Mineralogist, Volume 41(2), pages 273-291. https://doi.org/10.2113/gscanmin.41.2.273

Erdmer, P. and Williams, H.
1995: Grenville basement rocks (Humber Zone). In Geology of the Appalachian-Caledonian Orogen in Canada and Greenland. Geological Survey of Canada, Volume 6, pages 51-63.

Gehrels, G.E., Valencia, V.A. and Ruiz, J.
2008: Enhanced precision, accuracy, efficiency, and spatial resolution of U-Pb ages by laser ablation–multi-collector–inductively coupled plasma–mass spectrometry. Geochemistry, Geophysics, Geosystems, Volume 9(3). https://doi.org/10.1029/2007gc001805

Gower, C.F.
2019: Regional geology of eastern Labrador (eastern Makkovik and Grenville provinces). Government of Newfoundland and Labrador, Department of Natural Resources, Geological Survey, Memoir 4, 654 pages.

Heaman, L.M., Erdmer, P. and Owen, J.V.
2002: U–Pb geochronologic constraints on the crustal evolution of the Long Range Inlier, Newfoundland. Canadian Journal of Earth Sciences, Volume 39(5), pages 845-865. https://doi.org/10.1139/e02-015

Hinchey, A.M.
2010: Geology of the northern portion of the Silver Mountain map area (NTS 12H/11), southern Long Range Inlier, Newfoundland. *In* Current Research. Government of Newfoundland and Labrador, Department of Natural Resources, Geological Survey, Report 10-1, pages 245-263. https://doi.org/10.13140/RG.2.2.18689.07520

2020: Geology of the northern Silver Mountain map area (NTS 12H/11). Map 2020-18. Scale 1:50 000. Government of Newfoundland and Labrador, Department of Industry, Energy and Technology, Geological Survey, Open File 12H/11(2331). https://doi.org/10.13140/RG.2.2.18689.07520

Hinchey, A.M., Butler, J.P., Guilmette, C., Bédard, J.H., Fournierroy, F. and Coleman, M.
2023: Western Newfoundland: Allochthons, ophiolites and obduction. In Current Research. Government of Newfoundland and Labrador, Department of Industry, Energy and Technology, Geological Survey, Report 23-1, pages 163-180. https://doi.org/ 10.13140/RG.2.2.23440.48641

Hinchey, A.M., Knight, I., Sandeman, H.A. and Hinchey, J.G.
2022: Tournaisian volcanism associated with transtensional basin development in western Newfoundland during the amalgamation of Pangea. Gondwana Research, Volume 110, pages 226-248. https://doi.org/10.1016/j.gr.2022.06.013

Horn, I., Rudnick, R.L. and McDonough, W.F.
2000: Precise elemental and isotope ratio determination by simultaneous solution nebulization and laser ablation-ICP-MS: Application to U–Pb geochronology. Chemical Geology, Volume 164(3), pages 281-301. https://doi.org/https://doi.org/10.1016/S0009-2541(99)00168-0

Hyde, R.S., Miller, H.G., Hiscott, R.N. and Wright, J.A.
2007: Basin architecture and thermal maturation in the strike-slip Deer Lake Basin, Carboniferous of Newfoundland. Basin Research, Volume 1(2), pages 85-105. https://doi.org/10.1111/j.1365-2117.1988.tb 00007.x

Košler, J., Fonneland, H., Sylvester, P., Tubrett, M. and Pedersen, R.-B.
2002: U–Pb dating of detrital zircons for sediment provenance studies—a comparison of laser ablation ICPMS and SIMS techniques. Chemical Geology, Volume 182(2), pages 605-618. https://doi.org/10.1016/ S0009-2541(01)00341-2

Lock, B.E.
1969: Silurian Rocks of West White Bay Area, Newfoundland. *In* North Atlantic–Geology and Continental Drive. *Edited by* K. Marshall. American Association of Petroleum Geologists, Volume 12. https://doi.org/10.1306/M12367C33

Ludwig, K.R.
2003: User's Manual for Isoplot 3.00: A Geochronological Toolkit for Microsoft Excel.

Owen, J.V.
1991: Geology of the Long Range Inlier, Newfoundland. Geological Survey of Canada, Bulletin 395, 89 pages.

Rivers, T. and Murphy, B.
2012: Upper-crustal orogenic lid and mid-crustal core complexes: Signature of a collapsed orogenic plateau in the hinterland of the Grenville Province. Canadian Journal of Earth Sciences, Volume 49(1), pages 1-42. https://doi.org/10.1139/e11-014

Sandeman, H.A.I., Honsberger, I.W., Peddle, C., Kamo, S.L. and Dunning, G.R.
2024: Petrochemical and geochronological constraints on the origin of the Sops Arm group, the most westerly Silurian volcano-sedimentary extensional basin on the western Newfoundland composite Laurentian margin. Canadian Journal of Earth Sciences. e-First https://doi.org/10.1139/cjes-2024-0032

Smyth, W.R. and Schillereff, H.S.
1982: The Pre-Carboniferous geology of southwest White Bay. *In* Current Research. Government of Newfoundland and Labrador, Department of Mines and Energy, Mineral Development Division, Report 82-1, pages 78-98.

Sylvester, P.J. and Ghaderi, M.
1997: Trace element analysis of scheelite by excimer laser ablation-inductively coupled plasma-mass spectrometry (ELA-ICP-MS) using a synthetic silicate glass standard. Chemical Geology, Volume 141(1), pages 49-65. https://doi.org/https://doi.org/10.1016/S0009-2541(97)00057-0

van Staal, C.R. and Barr, S.M.
2012: Lithospheric architecture and tectonic evolution of the Canadian Appalachians and associated Atlantic margin. *In* Tectonic Styles in Canada: The LITHOPROBE Perspective. *Edited by* J.A. Percival, F.A. Cook and R.M. Clowes. Geological Association of Canada, Special Paper 49, pages 49-95.

van Staal, C.R., Barr, S.M., Waldron, J.W.F., Schofield, D.I., Zagorevski, A. and White, C.E.
2021: Provenance and Paleozoic tectonic evolution of Ganderia and its relationships with Avalonia and Megumia in the Appalachian-Caledonide orogen. Gondwana Research, Volume 98, pages 212-243. https://doi.org/10.1016/j.gr.2021.05.025

Vermeesch, P.
2023: Correction: Vermeesch, P. Exploratory Analysis of Provenance Data Using R and the Provenance Package. Minerals 2019, Volume 9, page 193. Minerals, Volume 13(3), page 375.
https://doi.org/10.3390/min13030375

Waldron, J.W.F., Barr, S.M., Park, A.F., White, C.E. and Hibbard, J.
2015: Late Paleozoic strike-slip faults in Maritime Canada and their role in the reconfiguration of the northern Appalachian orogen. Tectonics, Volume 34(8), pages 1661-1684.
https://doi.org/10.1002/2015tc003882

White, S.E., Waldron, J.W.F., Dunning, G.R. and Dufrane, S.A.
2019: Provenance of the Newfoundland Appalachian foreland basins. American Journal of Science, Volume 319(8), pages 694-735.
https://doi.org/10.2475/08.2019.03

Whitney, D.L. and Evans, B.W.
2010: Abbreviations for names of rock-forming minerals. American Mineralogist, Volume 95, pages 185-187.